NASA

Technical Memorandum **86131**

LARGE AMPLITUDE MHD WAVES UPSTREAM OF THE JOVIAN BOW SHOCK: REINTERPRETATION

Melvyn L. Goldstein
Hung K. Wong
Adolfo F. Vinas
Charles W. Smith

JULY 1984

National Aeronautics and
Space Administration

Goddard Space Flight Center
Greenbelt, Maryland 20771

LARGE AMPLITUDE MHD WAVES UPSTREAM OF THE JOVIAN BOW SHOCK: REINTERPRETATION

Melvyn L. Goldstein

Hung K. Wong*

Adolfo F. Viñas

Laboratory for Extraterrestrial Physics
NASA Goddard Space Flight Center

Charles W. Smith

Space Science Center
Department of Physics
University of New Hampshire

---

* NAS/National Research Council Resident Postdoctoral Associate

Abstract. Observations of large amplitude MHD waves upstream of the Jovian bow shock have previously been interpreted as arising from a resonant electromagnetic ion beam instability [Goldstein et al., 1983]. That interpretation was based on the conclusion that the observed fluctuations were predominantly right elliptically polarized in the solar wind rest frame. Because it has been noted by the authors that the fluctuations are, in fact, left elliptically polarized [Smith et al., 1984; Goldstein et al., 1984], a reanalysis of the observations is necessary. In this paper we investigate several mechanisms for producing left hand polarized MHD waves in the observed frequency range. Instabilities excited by protons appear unlikely to account for the observations. We conclude that a resonant instability excited by relativistic electrons escaping from the Jovian magnetosphere is a likely source of free energy consistent with the observations. Evidence for the existence of such a population of electrons has been found in both the Low Energy Charged Particle experiments and Cosmic Ray experiments on Voyager 2. This new interpretation is reminiscent of observations reported by Smith et al. [1976] using Pioneer data of left polarized (solar wind frame) MHD fluctuations in association with relativistic electrons.

1. Introduction

During a four day period from Day 180 to Day 184 (1979), as Voyager 2 approached Jupiter, large amplitude MHD fluctuations were observed in the magnetometer and plasma data. Detailed analysis of these data have been reported by Smith et al. [1983]. A subinterval, containing about one and a half hours of data from 900 to 1030 on Day 184, was analyzed by Goldstein et al. [1983] who argued that the fluctuations were produced by a wave-particle instability. Smith et al. [1983] had concluded that the fluctuations during this time interval were right elliptically polarized based on an argument which related the normalized magnetic helicity spectrum $\sigma_m(k)$ to the rest frame polarization (in the plasma physics convention, Stix [1962]) of MHD fluctuations. Given the right handed nature of the fluctuations, Goldstein et al. [1983] presented a Vlasov instability analysis suggesting that the observations resulted from an electromagnetic proton beam instability excited by solar wind protons reflected from the Jovian bow shock. The observed power spectra, frequency range, direction of minimum variance of the magnetic fluctuations all appeared to support this interpretation. A search of plasma data failed to reveal evidence of the required proton distribution. However, because the field of view of the plasma instrument was away from Jupiter during nearly all of this interval, it was unlikely that a reflected proton distribution could be detected.

In an erratum to their original paper, Smith et al. [1984] have pointed out that the relationship between magnetic helicity and plasma frame polarization given in the appendix of their paper is in error. This necessitates a new look at the interpretation of those observations given by Goldstein et al. [1983]. Based on the corrected relationship between

magnetic helicity and polarization found in Smith et al. [1984], we show in section 2 that the fluctuations observed on Day 184 are in fact left elliptically polarized and therefore cannot be excited by the resonant ion cyclotron instability originally considered. We then consider several alternative possibilities, including a nonresonant proton instability [Gary et al., 1984], and a resonant relativistic electron instability. In section 3, we show that the observations are best fit by assuming that the source of the observed fluctuations is relativistic electrons. The results are summarized in section 4.

2. A Reanalysis of Day 184

Goldstein et al. [1983], which we will often refer to as GSM, have presented a complete analysis of both the magnetic field and plasma data, and we will only summarize those results here. The magnetic field data is shown in field aligned coordinates in Figure 1 of that paper (and in RTN coordinates in Figure 9b of Smith et al. [1983]). The power spectrum of this hour and a half of magnetic field data shows a large peak at 2.3 mHz and several smaller peaks at 6, 9, and perhaps 12 mHz. The peak at 2.3 mHz is absent from the spectrum formed from the magnitude of the field (see Figure 2a and 2b of GSM). The normalized magnetic helicity spectrum, $\sigma_m(f)$ has large positive excursions at 2.3, 6, 9, and 12 mHz (Figure 3 of GSM). Due to its slower data collection rate, plasma data is limited to frequencies below 5 mHz. Between 2 - 3 mHz, the correlation between $|\underline{B}|$ and ρ is essentially zero, and the normalized cross helicity spectrum, $\sigma_c(f)$, is positive and nearly 0.5 (Figure 5 of GSM).

Because both $\sigma_m(f)$ and $\sigma_c(f)$ are positive near the peak of the spectrum

at 2.3 mHz, the plasma frame polarization (using the plasma physics convention, Stix [1962]) is left elliptical (see erratum by Smith et al. [1984] for details). As a further check on this conclusion, we show in Figure 1 a hodogram of a subset 100 9.6 s averaged magnetic field data points. The R-direction (and the direction of B_R) is into the plane of the paper. The abscissa and ordinate are the N and T directions, respectively. This is data as seen in the spacecraft frame. Note that in this frame of reference the sense of polarization is right-handed in the plasma physics convention. However, because these fluctuations are MHD waves and propagate with phase speeds less than the solar wind speed, they are being convected back past the spacecraft so that the plasma frame polarization is left-handed, in agreement with the polarization deduced from the normalized magnetic and cross helicity spectra. Because the Nyquist frequency of the plasma data is near 5 mHz, we cannot with certainty deduce the plasma frame polarization of magnetic fluctuations above 5 mHz. As a working hypothesis, we assume that since the magnetic helicity spectrum remains positive above 5 mHz, these fluctuations are also likely to be left elliptically polarized in the plasma frame.

One further assumption needs to be made, namely, that the source of free energy for producing these waves must originate either at the Jovian bow shock or within the Jovian magnetosphere. Thus, we will only consider wave-particle interactions in which the particles are streaming away from Jupiter. We know of only two plausible mechanisms that can excite left elliptically polarized MHD waves in this situation. The first is a nonresonant interaction with a diffuse suprathermal proton distribution. This instability has been analyzed for parallel propagation by Gary et al. [1984]. In this section and in Appendix A, the properties of this instability for oblique propagation are described. The second possibility, is that the waves are

being driven unstable by relativistic electrons. This instability has been previously cited by the Pioneer spacecraft investigators [Smith et al., 1976] as the origin of the waves observed in conjunction with the presence of relativistic electrons of Jovian origin. The basic analysis of this instability was developed by Dawson and Bernstein [1958], and Bernstein and Trehan [1960]. We will present a more complete description later in this section and in Appendix B.

To facilitate analysis of possible instabilities that can generate left elliptically polarized MHD fluctuations, we have developed a numerical code to solve the linearized Vlasov-Maxwell equations for a rather general class of specified distribution functions. This code is similar to the one used by Gary et al. [1984] and Forslund et al. [1979]. We have verified our numerical results by duplicating the results of the oblique analysis described in Gary et al. [1984]. An outline of the theoretical basis for the computer code is given in Appendix A.

In this section, we limit our discussion of the numerical solutions obtained from this code to instabilities that produce left hand polarized (plasma convention) waves propagating in the same direction as the proton beam and away from the Jovian bow shock. One general outcome of this analysis is the realization that, for the parameter range of interest, it is essential to use a warm plasma code. If solar wind protons were reflected from the Jovian bow shock in analogy to studies of similar phenomena at earth [Bonifazi and Moreno, 1981; Paschmann et al., 1980, 1981], the expected density of the resulting proton beam would be about 1%. This is large enough to modify significantly the real part of the wave dispersion relation [cf. Gary et al., 1981 and 1984]. In addition, the ratio of electron thermal energy to magnetic energy, β_e, is of order unity and this can change the sign

of wave polarization at large propagation angles.

We present results of this analysis only for the parameters previously used by GSM. In particular, we took $\beta_e = 1 = \beta_i$, where β_e and β_i are the electron and proton ratio of thermal to magnetic energy for the background solar wind plasma, $\beta_{i\parallel} = 30.9$ ($\beta_{i\perp} = 1113$) is the parallel (perpendicular) ratio of thermal to magnetic energy for the proton beam, $v_o = 50$ is the ion beam drift velocity normalized to the Alfvén speed $v_A = 14.4$ km/s, and $n_b/n_i = 0.01$, where n_b is the density of the proton beam and n_o is the ambient density. Note that the definitions of $\beta_{i\parallel}$ and $\beta_{i\perp}$ are $4\pi n_i KT_{i\parallel}$ and $4\pi n_i KT_{i\perp}$, where $T_{i\parallel}$ and $T_{i\perp}$ are the parallel and perpendicular temperatures of the proton beam, respectively.

Because the warm plasma dispersion relation is a transcendental equation, there are an indeterminant number of roots in the frequency and wavenumber range of interest. We found several left hand roots. Most of these were heavily damped and will not concern us further; one was a slow mode, which although unstable, did not occur in an appropriate frequency and wavenumber range, nor did it have an appropriate polarization and propagation direction. One unstable mode corresponded to the nonresonant proton instability discussed by Gary et al. [1984] (cf. Figure 10 of that paper). In Figure 2, the growth rate γ normalized by the proton cyclotron frequency Ω_i is shown as a function of wavenumber. The growth rate is plotted for wave propagation at 55°, 65°, and 75° to the mean magnetic field. Harmonic structure is not evident except at 75° where some evidence for a first harmonic is apparent. Note that below 55°, no growth is found. Above 75°, the harmonic structure disappears, and only a broad instability in wavenumber remains. The range of propagation angles for which this mechanism is unstable exceeds the minimum variance direction deduced for the observed fluctuations which was about 10°

for the fundamental and 30° - 40° for the harmonics.

Thus there is no evidence from linear Vlasov theory that a reflected proton beam can account for the observation of left polarized fluctuations with the observed harmonic structure and minimum variance directions. Recently, Krimigis et al. [1984] have reported that above 35 keV there is reason to believe that the flux of ions that is observed may be deficient in protons, especially near the Jovian bow shock. Recall that Goldstein et al. [1983] reported that there was no evidence of lower energy protons in the plasma data at this time. We therefore conclude that reflected protons are unlikely to be the origin of the observed MHD fluctuations.

3. Relativistic electrons

Coincident with the time interval during which the magnetic fluctuations were observed (0900 to 1030 UT on day 184 of 1979), Baker et al. [1984] have reported the presence of enhanced fluxes of energetic electrons (> 2.5 MeV). (Enhanced fluxes of energetic ions were present both before, during, and after the wave event.) The electron intensity began increasing at approximately 0900 UT, and reached a maximum at about 1030 UT when the MHD wave intensity began decreasing. In data from the Cosmic Ray experiment, kindly provided to us by E. C. Stone and A. C. Cummings (private communication), a large enhancement in relativistic electrons (energies in excess of 2.5 Mev) is observed to begin at 0900 UT and to end shortly after the MHD wave intensity decreases.

Neither tens of keV protons nor heavy ions can excite MHD waves in the observed frequency range. However, relativistic electrons can. Smith et al. [1976] noted that as Pioneer 10 approached the front side of the Jovian

magnetosphere, bursts of 3 - 6 MeV electrons were detected which were often accompanied by large amplitude magnetic fluctuations with frequencies close to 2 mHz (periods of ~ 10 min). They suggested that a likely explanation for their observations was that the electrons were exciting a cyclotron instability [Stix, 1962; Dawson and Bernstein, 1958]. This instability will produce left polarized waves in the solar wind frame. In this section, we explore the possibility that the waves observed in the Voyager 2 data could arise from such an instability.

The presence of harmonic structure in the power spectrum, together with the results of the minimum variance analysis, implies that an oblique instability is required. The analysis must be fully relativistic because electrons with several MeV energy are involved. In Appendix B we summarize the appropriate equations used in our analysis. Three simplifying assumptions were made in deriving the dispersion relation: the density of the electron beam must be much less than the ambient plasma density, the growth rate must be much less than the real part of the frequency, and the ambient plasma is cold. Because the energetic particle experiments cannot obtain detailed information about the distribution function of the electron beam, we have chosen parameters we believe to be reasonable and which best account for the observations. The streaming energy of the electrons is taken to be 2 MeV, which is also used for the perpendicular temperature of the energetic electron distribution. We used 200 keV for the parallel temperature. The importance of this anisotropy is discussed below. The growth rate is proportional to the ratio of n_s/n_o, where n_s is the density of the relativistic electron beam. In Figure 3 and the Table, this ratio is assumed to be 10^{-6}.

The results of our analysis are summarized in Figure 3 where the maximum

growth rate of the resonant left hand instability is plotted against $k_{\parallel}$. This growth rate has been maximized with respect to propagation direction, θ (or equivalently, $k_{\perp}$). Three harmonic peaks are clearly evident. The fundamental has maximum growth at $\theta = 0$, while the harmonics peak near 35°. This is in agreement with the minimum variance analysis reported by GSM. Adequate growth rates for the fundamental and harmonics can be obtained for density ratios between about 10^{-6} and 10^{-7}. It is important to note that the angle at which the harmonics peak is sensitive function of the temperature anisotropy of the electron beam; smaller anisotropies result in larger propagation directions. The fact that rather significant anisotropies are required to fit the observed minimum variance directions is puzzling because we know of no reason for expecting that relativistic electrons emanating from within the Jovian magnetosphere would have a perpendicular temperature that exceeded their parallel temperature. It is possible that the presence of harmonics in the power spectrum results from nonlinear mode coupling [Goldstein 1978], and may also represent wave steepening [Hoppe et al., 1981] rather than wave-particle resonances. However, the variation of the minimum variance direction with harmonic number reported by Goldstein et al. [1983] suggests a wave-particle origin for the harmonics.

We have also examined the resonant right hand instability using this electron distribution to ensure that the left hand instability is, in fact, the most important one in this frequency and wavenumber range. Those results are summarized in the Table. The growth rates for the left hand modes are greater than those for the right hand modes by factors of 3 - 4. The growth rate of whistler waves above the proton gyrofrequency is much less than the growth rate of the left hand mode. Excitation of Langmuir waves may be possible depending on the detailed shape of the electron distribution

function, but that electrostatic instability rapidly stabilizes via mode-coupling and does not extract significant energy from the energetic electrons [Smith et al., 1979; Goldstein et al., 1979].

4. Comparison with Electron Data

The low-energy charged-particle (LECP) detector on Voyager can detect electrons above 35 keV. Fifteen minute averages of these data from each of the eight angular sectors (including the background sector) were kindly supplied to us by K. M. Krimigis and B. Mauk. The data covered the time interval from 0400 to 1600 on day 184. We attempted to determine the parameters of the streaming two-temperature Maxwellian used in the linear instability analysis (v. appendix B) by using these data together with the fact that the particle intensity, J(E), is related to the distribution function $F_s(\underline{u})$ by $J \propto u^2 F$. At best this procedure can only be approximate because a streaming two-temperature Maxwellian is a poor fit to the observed intensity spectrum which is approximately a power law in kinetic energy.

Other systematic errors tend to reduce quantitative agreement between the model distributions and the data. For example, although the 350 keV and > 2.5 MeV channels (44 and 45, respectively) collect particles in a rather large opening angle (~ 60°), the magnetic field during this interval is tilted out the ecliptic at ~45°. Thus the LECP instrument may be missing a significant fraction of the incoming flux. In addition, the fluctuations in the magnetic field are at least as large as the mean, so that during the event the field is rotating in direction through a large angle. This tends to smear the distinction between "parallel" and "perpendicular" and will reduce the apparent anisotropies both streaming and thermal. Our goal in

this exercise is to determine characteristics of the electron distributions: first, whether there is evidence for a finite streaming anisotropy directed away from Jupiter and second, whether there is a thermal anisotropy with $\Psi_{s\perp}/\Psi_{s''} > 1$.

During this event, sector 1 of channels 44 and 45 looks along the nominal magnetic field direction (toward Jupiter). Similarly, sector 5 is directed away from the planet, and sectors 3 and 7 are looking approximately perpendicular to the field. The data from channels 44 and 45 in sector 3 (or sector 7) can be used to estimate $\Psi_{s\perp}$, the perpendicular thermal momentum per mass in units of c (see appendix B). The relationship is

$$\Psi_{s\perp}^2 = \frac{u_{44}^2 - u_{45}^2}{\ell n\{(u_{44}/u_{45})^2 \times [J_3(u_{45})/J_3(u_{44})]\}}$$

where $J_3(u_{45})$ and $J_3(u_{44})$ are the intensities in sector 3 in channels 45 and 44, respectively. u_{44} and u_{45} are the relativistic momenta per unit mass in units of c which correspond to 350 keV and 2.5 MeV, viz. $u_{44} = 1.4$ and $u_{45} = 5.8$.

By using the channel 44 and 45 data from both sectors 3 and 1, an expression for the streaming momentum in units of c, $u_{o''}$, can be obtained. The resulting expression is

$$u_{o''} = \frac{u_{44}^2 - u_{45}^2 \times [f(u_{44})/f(u_{45})]}{2\{u_{44} - u_{45} \times [f(u_{44})/f(u_{45})]\}}$$

where $f(u) = \ell n[J^1(u)/J^3(u)] - u^2/\Psi_{s\perp}^2$.

The remaining parameter, $\Psi_{s''}$, the parallel thermal momentum per mass (in units of c) can then be estimated from

$$\gamma_s''^2 = -(u_{\perp\perp}^2 - 2u_{\perp\perp}u_o'')/f(u_{\perp\perp})$$

Various other combinations of sectors and channel numbers can be used in the same way. The general results can be described as follows. Early in the event, at the time the magnetic fluctuations are first observed, the streaming anisotropy is maximum. It decreases to values consistent with zero as the event proceeds. From this approximate analysis we found a streaming energy of about 700 keV, somewhat less than the 2 MeV used in section 3. Throughout the event, the perpendicular temperature exceeds the parallel temperature, but the ratio is always less than 2 in contrast to the value of 10 used in section 3. However, the systematic errors described above all tend to decrease the estimated value of both the thermal and streaming anisotropies.

The observed intensity spectrum can be integrated to find an estimate of the density of the energetic electrons. Between 35 keV and 5 MeV, the density is $n_s \approx 8 \times 10^{-8}$ cm^{-3} (B. Mauk, private communication), which means that $n_s/n_o \approx 4 \times 10^{-7}$. This is close to the value $10^{-6} - 10^{-7}$ needed to account for the growth of the waves (see section 3).

We conclude that at least qualitatively, the LECP data are not inconsistent with the assumptions made in the instability analysis. The electrons are streaming away from Jupiter with a density adequate to excite the resonant instability. The perpendicular temperature is greater than the parallel temperature as is necessary to generate by wave-particle interactions the harmonics observed in the power spectrum. It should be kept in mind that the magnetic fluctuations have relatively large amplitudes and it

is therefore probable that nonlinear processes have caused evolution of the wave spectrum beyond that predicted by linear or quasi-linear theory. In particular, pitch angle scattering of the resonant electrons will tend to further reduce both the streaming and thermal anisotropies from the values required to initially excite the linear instability.

5. Summary and Conclusions

The reevaluation of the polarization of the large amplitude fluctuations observed upstream of Jupiter by Voyager 2, necessitated by the correction reported by Smith et al. [1984], has required a complete reinterpretation of the instability mechanism that can account for the observations. Streaming protons appear unable to generate left hand waves with the observed properties. Neither the resonant nor nonresonant proton instabilities can excite parallel propagating waves because the maximum growth rates always occur for oblique propagation and the waves are stable on axis. Harmonics can be excited by protons, but only at larger angles to the field than are consistent with the observed minimum variance directions. Finally, Krimigis et al. [1984] have reported that no evidence for the presence of energetic protons can be found in the LECP data during the time of these observations.

We have shown that relativistic electrons are capable of exciting MHD waves with the appropriate frequencies, wavenumbers, polarizations and propagation directions. Competing electron driven instabilities that might produce waves at higher frequencies (whistler waves or Langmuir waves) are found to be unimportant. The importance of relativistic electrons in generating MHD waves at millihertz frequencies was first noted by Smith et al.

[1976] in analyzing Pioneer 10 data. With the knowledge that the fluctuations observed by Voyager 2 were left polarized, it becomes clear that a similar phenomenon was probably being observed. This interpretation tends to be confirmed by the presence of large fluxes of 35 keV - 2 MeV electrons detected by both the LECP and Cosmic Ray experiments in near coincidence with the magnetometer observations. Finally, the density, streaming, and thermal anisotropies of the these electrons as estimated from the LECP data are qualitatively consistent with the requirements of the theory.

Appendix A

General Linear Dispersion Relation

The general dispersion relation for oblique propagation of plasma waves in a magnetized plasma can be found, e.g. in Harris [1961] and Tsai et al. [1981]. Our approach follows Tsai et al. [1981], but differs in that we restrict our attention to nonrelativistic protons. There are a few typographical errors in the matrix elements as published by Tsai et al. which are corrected in the summary given here. The background magnetic field $\underline{B}_0$ is assumed to be in the z-direction. The general dispersion relation can be written as:

$$D_{ij}(\underline{k},\omega) = (1 - \frac{k^2c^2}{\omega^2})\,\delta_{ij} + \frac{c^2}{\omega^2}\,k_i k_j$$

$$+ 2\pi \sum_\alpha \frac{\omega_\alpha^2}{\omega^2} \int_{-\infty}^{+\infty} dv_\parallel \int_0^\infty dv_\perp\, v_\perp \left[v_\perp \frac{\partial f_\alpha}{\partial v_\parallel} - v_\parallel \frac{\partial f_\alpha}{\partial v_\perp} \right] \hat{e}_z \hat{e}_z$$

$$- 2\pi \sum_\alpha \sum_{n=-\infty}^{+\infty} \frac{\omega_\alpha^2}{\omega^2} \int_{-\infty}^{+\infty} dv_\parallel \int_0^\infty dv_\perp \frac{(T_\alpha^{(n)})_{ij}}{k_\parallel v_\parallel + n\Omega_\alpha - \omega} \times$$

$$\{\omega \frac{\partial f_\alpha}{\partial v_\perp} + k_\parallel [v_\perp \frac{\partial f_\alpha}{\partial v_\parallel} - v_\parallel \frac{\partial f_\alpha}{\partial v_\perp}]\} \qquad \text{(A1)}$$

where the tensor $(T_\alpha^{(n)})_{ij}$ is defined by

$$(T_\alpha^{(n)})_{ij} =$$

$$\begin{pmatrix} \frac{n^2\Omega_\alpha^2}{k_\perp^2}J_n^2 & \frac{in\Omega_\alpha}{k_\perp}v_\perp J_n J_n' & \frac{n\Omega_\alpha}{k_\perp}v_\parallel J_n^2 \\ -\frac{in\Omega_\alpha}{k_\perp}v_\perp J_n J_n' & v_\perp^2 (J_n')^2 & -iv_\parallel v_\perp J_n J_n' \\ \frac{n\Omega_\alpha}{k_\perp}v_\parallel J_n^2 & iv_\parallel v_\perp J_n J_n' & v_\parallel^2 J_n^2 \end{pmatrix}$$

$J_n = J_n(k_\perp v_\perp/\Omega_\alpha)$ is the Bessel function of order n and J_n' is its derivative. The square of the plasma frequency of the αth species is $\omega_\alpha^2 = (4\pi n_\alpha q_\alpha^2/m_\alpha)$, q_α is the charge of the αth species, and the gyrofrequency is $\Omega_\alpha = q_\alpha B_o/m_\alpha c$. If we limit our attention to equilibrium distribution functions that are streaming bi-Maxwellians, then f_α has the form:

$$f_\alpha = (\pi^{3/2}\psi_{\alpha\perp}^2\psi_{\alpha\parallel})^{-1} \exp[-(v_\perp^2/\psi_{\alpha\perp}^2) - (v_\parallel - v_{o\alpha})^2/\psi_{\alpha\parallel}^2] \qquad \text{(A2)}$$

where $\psi_{\alpha\perp,\parallel} = (KT_{\alpha\perp,\parallel}/m_\alpha)^{1/2}$ and K is Boltzmann's constant.

The choice (A2) for the generic form of the distribution functions permits the integrals in (A1) to be done analytically. The integration over $v_\perp$ is performed first using the identities

$$\int_0^\infty dx\, x\, J_n^2(x) \exp(-x^2/2\lambda) = \lambda\, \Lambda_n(\lambda)$$

$$\int_0^\infty dx\, x^2\, J_n(x)\, J_n'(x)\, \exp(-x^2/2\lambda) = \lambda^2\, \Lambda_n'(\lambda)$$

$$\int_0^\infty dx\, x^3\, [J_n'(x)]^2\, \exp(-x^2/2\lambda) = n^2\lambda\Lambda_n(\lambda) - 2\lambda^3\Lambda_n'(\lambda)$$

where $\Lambda_n(\lambda) = \exp(-\lambda)\, I_n(\lambda)$, and $I_n(\lambda)$ is the modified Bessel function, and Λ_n' is the derivative with respect to λ.

The integrals over $v_\parallel$ can be written in terms of the plasma dispersion function

$$Z(\xi_\alpha) = (1/\sqrt{\pi}) \int_{-\infty}^{+\infty} dx\, \exp(-x^2) \,/\, (x - \xi_\alpha)$$

where

$$\xi_\alpha = (\omega - k_\parallel v_{o\alpha} - n\Omega_\alpha)/(k_\parallel \Psi_{\alpha\parallel})$$

After some elementary, but tedious algebra, the dispersion tensor can be rewritten in the form

$$D_{ij}(\underline{k},\omega) =$$

$$\begin{pmatrix} 1 - \frac{k_{\shortparallel}^2 c^2}{\omega^2} + Q_{xx} & Q_{xy} & \frac{c^2 k_{\shortparallel} k_{\perp}}{\omega^2} + Q_{xz} \\ Q_{yx} & 1 - \frac{c^2 k^2}{\omega^2} + Q_{yy} & Q_{yz} \\ \frac{c^2 k_{\shortparallel} k_{\perp}}{\omega^2} + Q_{zx} & Q_{zy} & 1 - \frac{c^2 k_{\perp}^2}{\omega^2} + Q_{zz} \end{pmatrix} \tag{A3}$$

where the Q_{ij} are defined by

$$Q_{xx} = 2\sum_{\alpha}\sum_{n} \frac{\omega_{\alpha}^2}{\omega^2} \Lambda_n \frac{n^2\Omega_{\alpha}^2}{k_{\perp}^2 \psi_{\alpha\perp}^2} [(\mu_{\alpha} - 1) + \mu_{\alpha}\bar{\xi}_{\alpha} Z(\xi_{\alpha})]$$

$$Q_{xy} = 2i\sum_{\alpha}\sum_{n} \frac{\omega_{\alpha}^2}{\omega^2} (\lambda_{\alpha}\Lambda'_n/2)\, \mu_{\alpha}\bar{\xi}_{\alpha} Z(\xi_{\alpha})$$

$$Q_{yx} = -Q_{xy}$$

$$Q_{xz} = 2\sum_{\alpha}\sum_{n} \frac{\omega_{\alpha}^2}{\omega^2} \Lambda_n \frac{n\Omega_{\alpha}}{k_{\perp}\psi_{\alpha\shortparallel}} [(1/\mu_{\alpha} - 1)\frac{n\Omega_{\alpha}}{k_{\shortparallel}\psi_{\alpha\shortparallel}} +$$

$$y_{\alpha}\bar{\xi}_{\alpha} Z(\xi_{\alpha})]$$

$$Q_{yy} = 2\sum_{\alpha}\sum_{n} \frac{\omega_\alpha^2}{\omega^2} \frac{\Omega_\alpha^2}{k_\perp^2 \Psi_{\alpha\perp}^2} (n^2\Lambda_n - 2\lambda_\alpha^2\Lambda'_n)[(\mu_\alpha - 1) +$$

$$\mu_\alpha \bar{\xi}_\alpha Z(\xi_\alpha)]$$

$$Q_{yz} = -2i\sum_{\alpha}\sum_{n} \frac{\omega_\alpha^2}{\omega^2} \frac{\Omega_\alpha \lambda_\alpha}{k_\perp \Psi_{\alpha\parallel}} \Lambda'_n \, y_\alpha \bar{\xi}_\alpha Z(\xi_\alpha)$$

$$Q_{zx} = Q_{xz}$$

$$Q_{zy} = -Q_{yz}$$

$$Q_{zz} = 2\sum_{\alpha}\sum_{n} \frac{\omega_\alpha^2}{\omega^2} \Lambda_n \left[\left(\frac{\omega}{k_\parallel \Psi_{\alpha\parallel}}\right)^2 + (1 - 1/\mu_\alpha)\left(\frac{n\Omega_\alpha}{k_\parallel \Psi_{\alpha\parallel}}\right)^2\right.$$

$$\left. + y_\alpha^2 \bar{\xi}_\alpha Z(\xi_\alpha)\right] \qquad \text{(A5)}$$

where $\mu_\alpha = \Psi_{\alpha\perp}^2/\Psi_{\alpha\parallel}^2$, $\bar{\xi}_\alpha = \{\omega - k_\parallel v_{o\alpha} - [1 - (\mu_\alpha)^{-1}]n\Omega_\alpha\}/(k_\parallel \Psi_{\alpha\parallel})$, $\xi = (\omega - k_\parallel v_{o\alpha} - n\Omega_\alpha)/(k_\parallel \Psi_{\alpha\parallel})$, and $y_\alpha = (\omega - n\Omega_\alpha)/(k_\parallel \Psi_{\alpha\parallel})$. A useful identity for numerical evaluation of the complex roots of (A5) is

$$\Lambda'_n(\lambda_\alpha) = \Lambda_{n-1}(\lambda_\alpha) - (1 + n/\lambda_\alpha)\Lambda_n(\lambda_\alpha)$$

Appendix B

Relativistic Electron Instability

To derive the growth rates of MHD waves excited by relativistic electrons, we assume that the density of the electrons is much less than that of the background plasma. Thus, the relativistic electrons only contribute to the growth of the waves and do not modify the real part of the wave dispersion relation.

In the limit $\gamma \ll \omega$, the growth rate of low frequency MHD waves as determined from the linearized Vlasov-Maxwell equations is given by [Stix, 1962; Kennel and Wong, 1967; Tademaru, 1969]

$$\gamma = - R^i/(\partial R^r/\partial\omega) \qquad (B1)$$

where R^r is the real part of the determinant of the dispersion tensor (computed in this case using the cold plasma approximation). R^i is the imaginary part of the determinant of the dispersion tensor which comes from the lowest order contribution of the relativistic electrons. After some elementary but tedious algebra, the expression for γ can be written as [Freund et al., 1983]

$$\gamma = 2\pi^2 \frac{\omega_s^2}{G\omega} \int_{-\infty}^{\infty} du_\parallel \int_0^{\infty} du_\perp \frac{u_\perp}{\Gamma} \sum_{n=-\infty}^{\infty} \frac{n\Omega_e}{k_\perp} \times$$

$$\left[n\Omega_e \frac{\partial}{\partial u_\perp} + k_\parallel u_\perp \frac{\partial}{\partial u_\parallel}\right] F_s(u_\perp, u_\parallel) \times$$

$$\left\{\left[\psi_{11} + \psi_{22} + \psi_{12} + \frac{k_\perp^2 u_\parallel^2}{n^2\Omega_e^2}\psi_{33} + \frac{k_\perp u_\parallel}{n\Omega_e}(\psi_{13} - \psi_{23})\right]\frac{n}{b}J_n^2(b)\right.$$

$$- [2\psi_{22}+\psi_{12} - \frac{k_\perp u_\perp}{n\Omega_e}\psi_{23}]J_n(b)J_{n+1}(b) + \frac{b}{n}\psi_{22}J_{n+1}{}^2(b)\}$$

$$\times \delta(\Gamma\omega - n\Omega_e - k_\parallel u_\parallel) \qquad (B2)$$

where $\omega_s{}^2 = 4\pi n_s e^2/m_e$; n_s and m_e denote the density and rest mass of the relativistic electrons, respectively; $\underline{u} \equiv \underline{P}/m_e$ is the momentum per unit mass; $\Gamma \equiv (1 + u^2/c^2)^{1/2}$; $b \equiv k_\perp u_\perp/\Omega_e$; $\Omega_e \equiv |e|B_o/m_e c$; ψ_{ij} are given by

$$\psi_{11} \equiv N^4\sin^2\theta - N^2(\varepsilon\sin^2\theta + \eta) + \varepsilon\eta$$

$$\psi_{22} \equiv \varepsilon\eta - N^2(\varepsilon\sin^2\theta + \eta\cos^2\theta)$$

$$\psi_{33} \equiv N^4\cos^2\theta - N^2\varepsilon(1 + \cos^2\theta) + \varepsilon^2 - g^2$$

$$\psi_{12} \equiv 2g(\eta - N^2\sin^2\theta)$$

$$\psi_{23} \equiv 2N^2 g\sin\theta\cos\theta$$

$$\psi_{13} \equiv 2N^2(N^2 - \varepsilon)\sin\theta\cos\theta$$

with

$$\varepsilon \equiv 1 - \frac{\omega_e{}^2}{\omega^2 - \Omega_e{}^2} - \frac{\omega_i{}^2}{\omega^2 - \Omega_i{}^2}$$

$$\eta \equiv 1 - \frac{\omega_e{}^2}{\omega^2} - \frac{\omega_i{}^2}{\omega^2}$$

$$g \equiv \frac{\omega_e{}^2\Omega_e}{\omega(\omega^2 - \Omega_e{}^2)} - \frac{\omega_i{}^2\Omega_i}{\omega(\omega^2 - \Omega_i{}^2)}$$

$$N \equiv kc/\omega$$

and

$$G \equiv \omega\, \partial R^r/\partial\omega$$

$$= (\omega \frac{\partial \varepsilon}{\partial \omega} \sin^2\theta + \omega \frac{\partial \eta}{\partial \omega} \cos^2\theta)\, N^4 +$$

$$N^2\{-2[(\varepsilon^2 - g^2)\sin^2\theta + \varepsilon\eta(1 + \cos^2\theta)]$$

$$-2(\varepsilon\omega\partial\varepsilon/\partial\omega - g\omega\partial g/\partial\omega)\sin^2\theta$$

$$-(\eta\omega\partial\varepsilon/\partial\omega + \varepsilon\omega\partial\eta/\partial\omega)(1 + \cos^2\theta)\}$$

$$+ (4\eta + \omega\partial\eta/\partial\omega)(\varepsilon^2 - g^2) + 2\eta(\varepsilon\omega\partial\varepsilon/\partial\omega - g\omega\partial g/\partial\omega)$$

where

$$\omega\partial\varepsilon/\partial\omega = 2\omega^2[\frac{\omega_e^2}{(\omega^2 - \Omega_e^2)^2} - \frac{\omega_i^2}{(\omega^2 - \Omega_i^2)^2}]$$

$$\omega\partial\eta/\partial\omega = 2(\frac{\omega_e^2}{\omega^2} + \frac{\omega_i^2}{\omega^2})$$

$$\omega\partial g/\partial\omega = -2\omega[\frac{\omega_e^2\Omega_e}{(\omega^2 - \Omega_e^2)^2} - \frac{\omega_i^2\Omega_i}{(\omega^2 - \Omega_i^2)^2}] - g$$

In the above expressions, ω_e and ω_i are the plasma frequencies of the background electrons and ions, respectively.

In performing the stability analysis, the unperturbed distribution function of the relativistic electrons, $F_s(u_\perp, u_\parallel)$, is assumed to have the form

$$F_s(u_\perp, u_\parallel) = \frac{1}{(\pi^{3/2} \psi_{s\perp}^2 \psi_{s\parallel})} \exp -(u_\perp^2/\psi_{s\perp}^2) \times$$

$$\exp -(u_\parallel - u_{o\parallel})^2/\psi_{s\parallel}^2$$

Acknowledgments. This work was supported, in part, by the NASA Solar Terrestrial Theory Program grant to the Goddard Space Flight Center. The work of C. W. Smith was supported, in part, by the NASA STTP grant to the University of New Hampshire. The authors would like to express their appreciation to E. C. Stone and A. C. Cummings for providing us with the Voyager 2 cosmic ray electron data and to S. M. Krimigis and B. Mauk for providing us with the Voyager 2 low energy electron data from the LECP experiment. M. Acuña, M. Lee, S. P. Gary, S. M. Krimigis, B. Mauk are thanked for many stimulating discussions.

References

Baker, D. N., R. D. Zwickl, S. M. Krimigis, J. F. Carbary, and M. H. Acuña, Energetic particle acceleration and transport in the upstream region of Jupiter: Voyager results, J. Geophys. Res., submitted, 1984.

Bernstein, I. B., and S. K. Trehan, Plasma oscillations (1), Nucl. Fusion, 1, 3, 1960.

Bonifazi, C., and G. Moreno, Reflected and diffuse ions backstreaming from the earth's bow shock, 2, Origin, J. Geophys. Res., 86, 4405, 1981.

Dawson, J., and I. B. Bernstein, Hydromagnetic instabilities caused by runaway electrons, Controlled Thermonuclear Conference, Rep. AED-TID-7558, p. 360, Dep. of Commer., Washington, D. C., 1958.

Forslund, D. W., J. M. Kindel, and M. A. Stroscio, Current driven electromagnetic ion cyclotron instability, J. Plasma Phys., 21, 127, 1979.

Freund, H. P., H. K. Wong, C. S. Wu, and M. J. Xu, An electron cyclotron maser instability for astrophysical plasmas, Phys. Fluids, 26, 2263 1983.

Gary, S. P., C. W. Smith, M. A. Lee, M. L. Goldstein, and D. W. Forslund, Electromagnetic ion beam instabilities, Phys. Fluids, in press, 1984.

Goldstein, M. L., An instability of finite amplitude circularly polarized Alfvén waves, The Astrophys. J., 219, 700, 1978.

Goldstein, M. L., C. W. Smith, and W. H. Matthaeus, Large amplitude MHD waves upstream of the Jovian Bow shock, J. Geophys. Res., 88, 9989, 1983.

Goldstein, M. L., C. W. Smith, and W. H. Matthaeus, Correction to "Large amplitude MHD waves upstream of the Jovian Bow shock", J. Geophys. Res., in press, 1984.

Goldstein, M. L., R. A. Smith, and K. Papadopoulos, Nonlinear stability of

solar type III radio bursts. II. Application to observations near 1 AU, The Astrophys. J., 234, 683, 1979.

Harris, E. G., Plasma instabilities associated with anisotropic velocity distributions, J. Nuclear Energy C, 2, 138, 1961.

Hoppe, M. M., C. T. Russell, L. A. Frank, T. E. Eastman, and E. W. Greenstadt, Upstream hydromagnetic waves and their association with backstreaming ion populations: ISEE 1 and 2 observations, J. Geophys. Res., 86, 4471, 1981.

Kennal, C. F., and H. V. Wong, Resonant particle instabilities in a uniform magnetic field, Plasma Phys., 1, 75, 1967.

Krimigis, S. M., E. T. Sarris, R. D. Zwickl, and D. N. Baker, Energetic ions upstream of Jupiter's bow shock, J. Geophys. Res., submitted, 1984.

Paschmann, G., N. Sckopke, J. R. Asbridge, S. J. Bame, and J. T. Gosling, Energization of solar wind ions by reflection from the earth's bow shock, J. Geophys. Res., 85, 4689, 1980.

Paschmann, G., N. Sckopke, I. Papamastorakis, J. R. Asbridge, S. J. Bame, and J. T. Gosling, Characteristics of reflected and diffuse ions upstream from the earth's bow shock, J. Geophys. Res., 86, 4355, 1981.

Smith, C. W., M. L. Goldstein, and W. H. Matthaeus, Turbulence analysis of the Jovian upstream 'wave' phenomenon, J. Geophys. Res., 88, 5581, 1983.

Smith, C. W., M. L. Goldstein, W. H. Matthaeus, and A. F. Viñas, Correction to "Turbulence analysis of the Jovian upstream 'wave' phenomenon", J. Geophys. Res., in press, 1984.

Smith, E. J., B. T. Tsurutani, D. L. Chenette, T. F. Conlon, and J. A. Simpson, Jovian electron bursts: Correlation with the interplanetary field direction and hydromagnetic waves, J. Geophys. Res., 81, 65, 1976.

Smith, R. A., M. L. Goldstein, and K. Papadopoulos, Nonlinear stability of

solar type III radio bursts. I. Theory, The Astrophys. J., 234, 348, 1979.

Stix, T. H., The Theory of Plasma Waves, McGraw-Hill, New York, 1962.

Tademaru, E., Plasma instabilities of streaming cosmic rays, The Astrophys. J., 158, 959, 1969.

Tsai, S. T., C. S. Wu, Y. D. Wang, and S. W. Kang, Dielectric tensor of a weakly relativistic, nonequilibrium, and magnetized plasma, Phys. Fluids, 24, 2186 1981.

M. L. Goldstein, Code 692, Laboratory for Extraterrestrial Physics, NASA Goddard Space Flight Center, Greenbelt, MD 20771.

C. W. Smith, Space Science Center, Department of Physics, University of New Hampshire, Durham, NH 03824.

A. F. Viñas, Code 692, Laboratory for Extraterrestrial Physics, NASA Goddard Space Flight Center, Greenbelt, MD 20771.

H. K. Wong, Code 692, Laboratory for Extraterrestrial Physics, NASA Goddard Space Flight Center, Greenbelt, MD 20771.

Table. Relativistic Electron Instability:

Growth Rates for the Alfvén and Fast Modes

Harmonic number n	Alfvén Mode $(\gamma/\Omega_i)_{max}$	Propagation direction θ	Fast Mode $(\gamma/\Omega_i)_{max}$	Propagation direction θ
1	0.135	0°	0.034	21°
2	0.014	35°	0.0038	55°
3	0.0059	33°	0.0018	51°

A density ratio of 10^{-6} is assumed.

Figure Captions

Figure 1. Hodogram of the magnetic field during the time interval when the large amplitude waves are present. The radial direction is into the plane of the figure. This is also the direction of the radial component of the magnetic field. Note that these fluctuations are right hand in the space craft frame of reference.

Figure 2. Proton instability for the left hand mode. ρ_i is the proton Larmor radius. Below 55°, the left hand mode is stable. Above 75°, the instability exhibits no harmonic structure.

Figure 3. Relativistic electron instability for the left hand mode plotted as a function of parallel wavenumber. The growth rate has been maximized with respect to propagation direction. Clear evidence for a fundamental and at least two harmonics is present. $n_s/n_o = 10^{-6}$ has been assumed, but the growth rate is directly proportional to this ratio. The streaming energy and the perpendicular temperature of the electrons is 2 Mev, the parallel temperature is 200 keV.

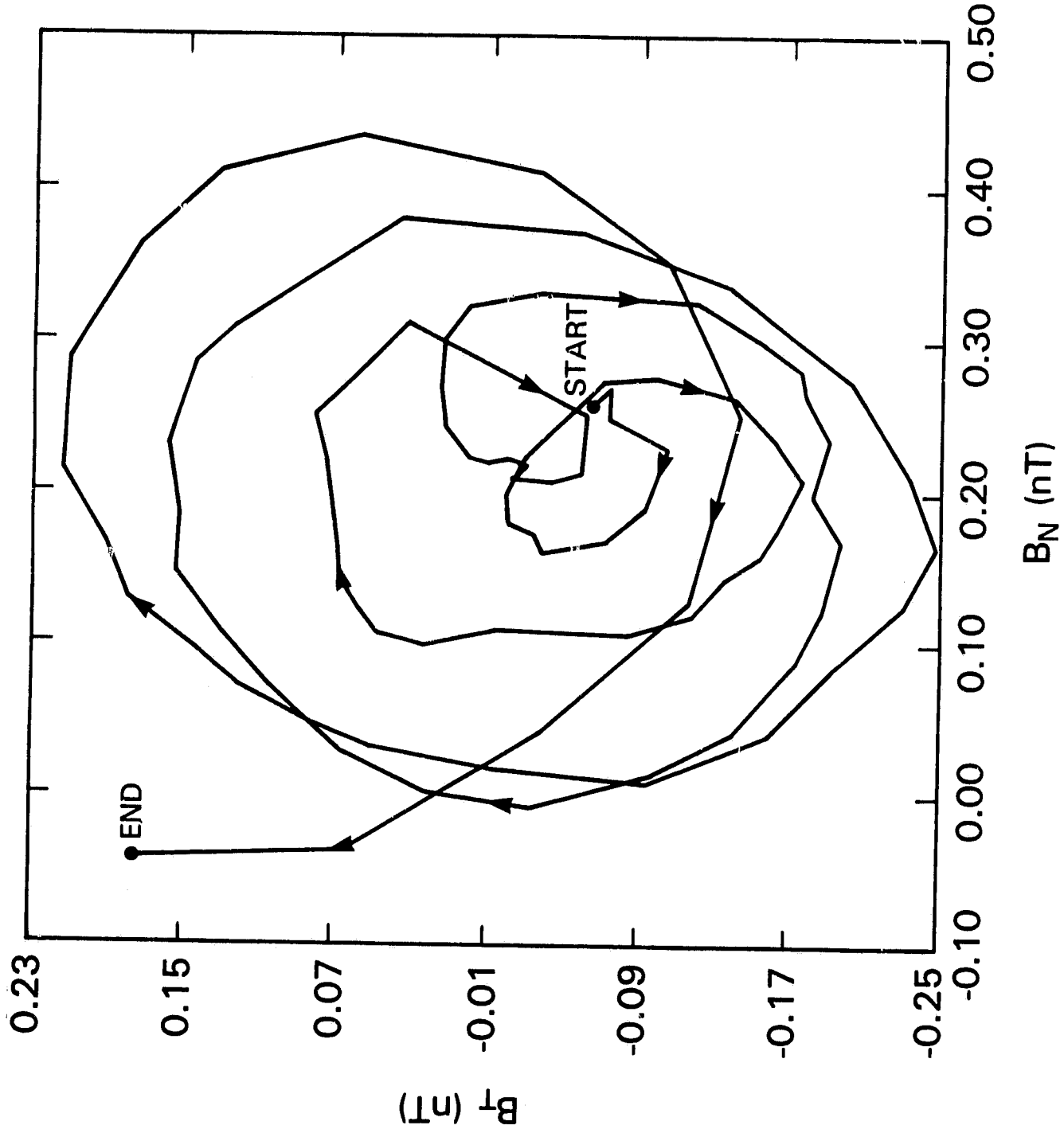

Figure 1

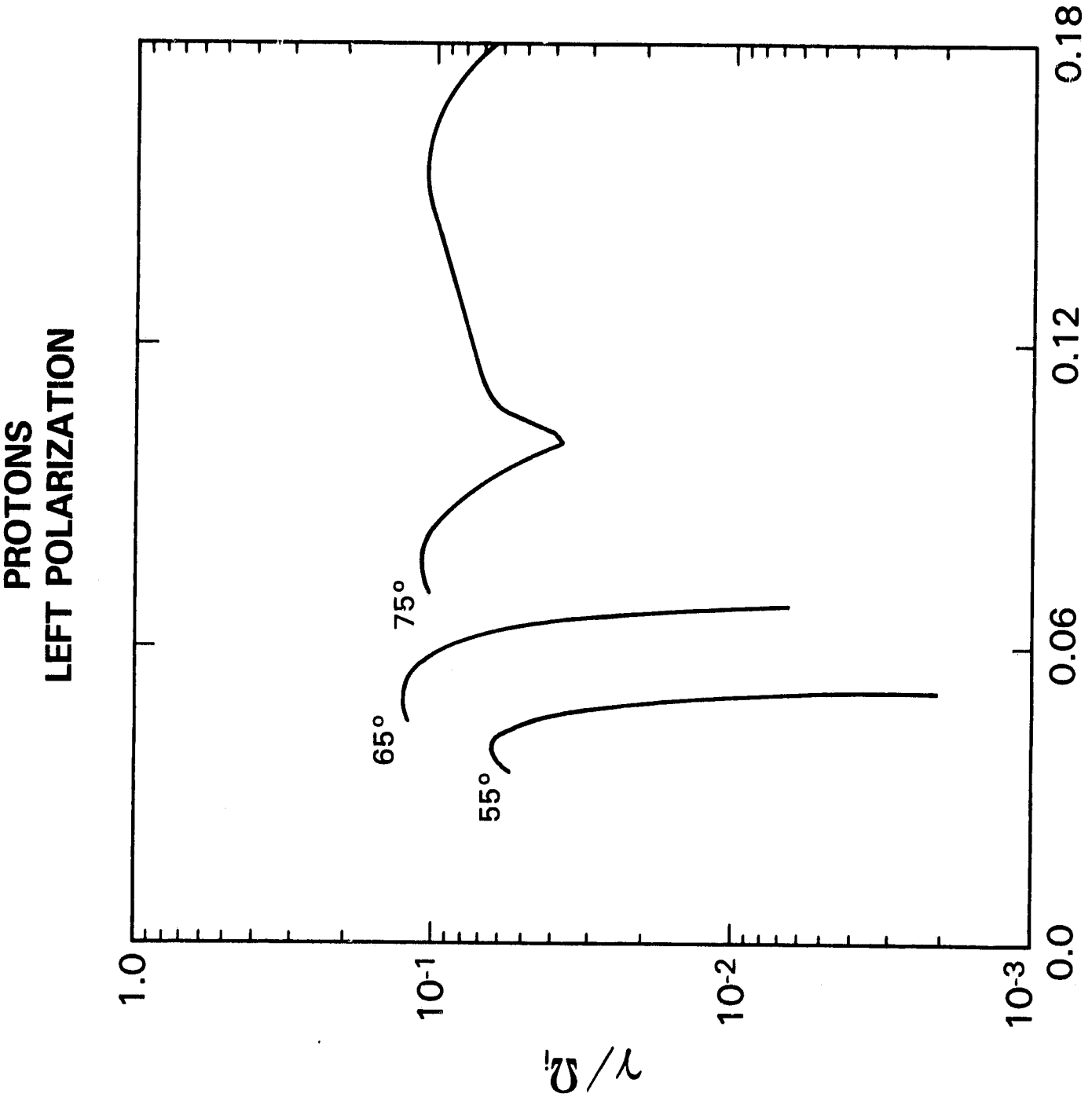

Figure 2

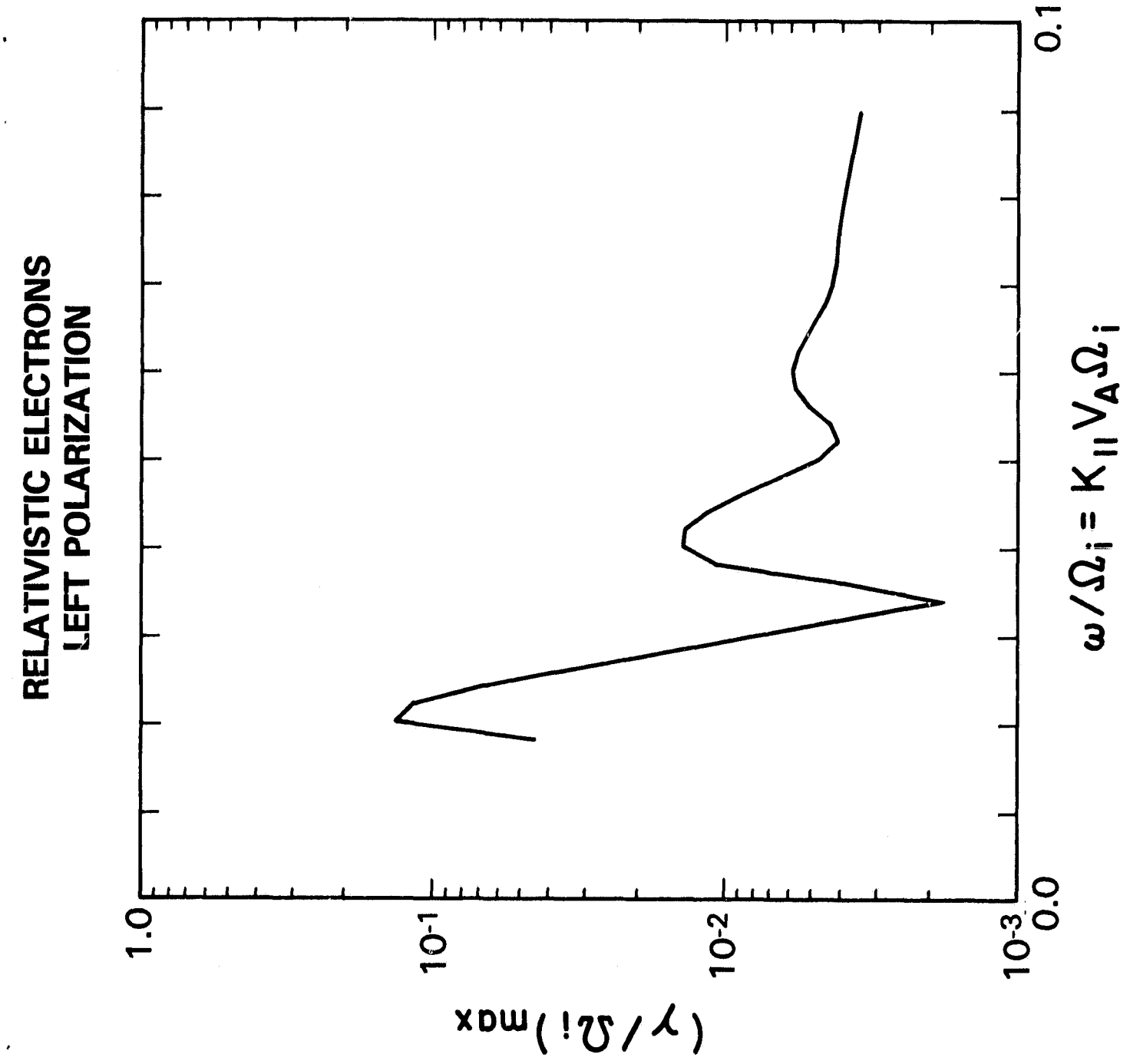

Figure 3